Adv. Appl. Prob. (SGSA) **40,** 630–650 (2008)
Printed in Northern Ireland

RANDOM LAGUERRE TESSELLATIONS

CLAUDIA LAUTENSACK,* *University of Applied Sciences, Darmstadt*
SERGEI ZUYEV,** *University of Strathclyde*

Abstract

A systematic study of random Laguerre tessellations, weighted generalisations of the well-known Voronoi tessellations, is presented. We prove that every normal tessellation with convex cells in dimension three and higher is a Laguerre tessellation. Tessellations generated by stationary marked Poisson processes are then studied in detail. For these tessellations, we obtain integral formulae for geometric characteristics and densities of the typical k-faces. We present a formula for the linear contact distribution function and prove various limit results for convergence of Laguerre to Poisson–Voronoi tessellations. The obtained integral formulae are subsequently evaluated numerically for the planar case, demonstrating their applicability for practical purposes.

Keywords: Laguerre tessellation; power tessellation; weighted Voronoi tessellation; k-face density; Poisson process; random tessellation; stochastic geometry

2000 Mathematics Subject Classification: Primary 60D05; 60G55
Secondary 05B45; 52A22; 62H11

1. Introduction

Random tessellations are widely used to model natural cellular structures ranging from organic tissues to telecommunication networks to the origins of the universe. Perhaps the most popular model is the *Voronoi tessellation* in $\mathbb{R}^d$ which is defined by an at most countable set of distinct 'generator' points or *nuclei* $\varphi = \{x_1, x_2, \dots\} \subset \mathbb{R}^d$ as follows. With each $x_i \in \varphi$, there is associated a *cell* $C(x_i, \varphi)$ consisting of the points of $\mathbb{R}^d$ which are closer to x_i than to any other $x_j \in \varphi$. Being the intersection of half-spaces, i.e.

$$C(x_i, \varphi) = \bigcap_{x_j \in \varphi} \{y \in \mathbb{R}^d : \|y - x_i\| \le \|y - x_j\|\}, \tag{1.1}$$

all the cells are nonempty polytopes and it is also customary to call x_i the *centre* or *centroid* of the cell $C_i = C(x_i, \varphi)$, meaning that there is a one-to-one correspondence between the cells and φ. In the case when the nuclei set is a random point process Φ, the tessellation $\{C(x, \Phi) : x \in \Phi\}$ becomes a random object, too, and it is usually described by means of the random closed set of the cells' boundaries. In particular, when Φ is a homogeneous Poisson process, we speak of the *Poisson–Voronoi tessellation*. A multitude of results is available for both nonrandom and random Voronoi tessellations. A comprehensive account of these can be found in the monographs [7] and [20].

Received 28 November 2007; revision received 17 March 2008.
* Postal address: Fraunhofer ITWM, Fraunhofer-Platz 1, 67663 Kaiserslautern, Germany.
Email address: claudia.lautensack@itwm.fraunhofer.de
** Postal address: Department of Statistics and Modelling Science, University of Strathclyde, 26 Richmond Street, Glasgow G1 1XH, UK. Email address: sergei@stams.strath.ac.uk

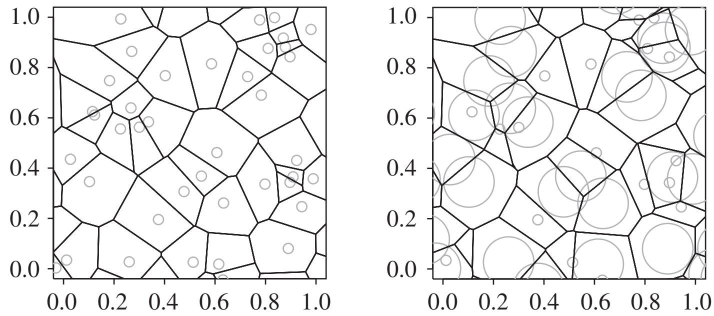

FIGURE 1: A Poisson–Voronoi tessellation in $\mathbb{R}^2$ (*left*) and the Laguerre tessellation of the same set of points with radii chosen from a two-atom distribution (*right*). Note how the cell geometry is altered by the introduction of weights, that some Laguerre cells are empty (around position (0.3, 0.6) or (0.9, 0.3)), and that some cells do not contain the nucleus (for instance, the almost triangular cell at (0.1, 0.1)).

Although Voronoi tessellations proved extremely useful in modelling many natural phenomena, in some situations they may still be too restrictive. In particular, the cell geometry depends entirely on the mutual position and the distances between the nuclei; in this respect all the nuclei bear the same 'weight'. But we can also envisage practical scenarios when different nuclei have different 'power', so that the more powerful has a bigger cell. This idea leads to the replacement of the Euclidean norm in (1.1) by a *power distance*. Namely, if each nucleus x_i has an associated weight w_i then the new cells are defined to be

$$C_i = \bigcap_{(x_j, w_j) \in \varphi} \{y \in \mathbb{R}^d \colon \operatorname{pow}(y, (x_i, w_i)) \le \operatorname{pow}(y, (x_j, w_j))\},$$

where $\operatorname{pow}(y, (x, w)) = \|y - x\|^2 - w$. If w is positive then it is indeed the power of the point y with respect to a sphere $s(x, r)$ centred in x with radius $r = \sqrt{w}$, hence the name. In this paper we mainly consider the case of positive weights and label the nuclei x_i with these radii r_i rather than with w_i.

The power distance has been considered by several authors [6], [8], [9]. The first analyses of the corresponding *deterministic* tessellations seem to be [1], [3], and [11]. Often these tessellations are called *power tessellations*; however, the synonym *Laguerre tessellations* has also been established and will be used in this paper.

It is clear that when all weights are the same, the Laguerre tessellation *is* the Voronoi tessellation. When they are not, much similarity to the Voronoi case still remains: the cells are all polytopes and, under some mild regularity assumptions of general position type imposed on the nuclei, the Laguerre tessellation is also *normal*, i.e. each k-dimensional face lies in the intersection of exactly $d - k + 1$ cells (vertices are zero-dimensional faces). But there are also differences, the most striking, perhaps, are that a nucleus may not be contained in its cell and that a Laguerre cell may be empty. Hence, for Laguerre tessellations, the notions of nuclei and cell centroids *are* different; see Figure 1.

In this paper the authors present the first systematic study of random Laguerre tessellations. The next section contains notation and formal definitions of the objects we will be dealing with: tessellations, their general properties, and their moment characteristics. In Section 3 we establish important topological properties of Laguerre tessellations and state that every normal tessellation in dimension three and higher is a Laguerre tessellation. The proof of this new result is given in Appendix A. Section 4 concentrates on Poisson–Laguerre tessellations. We first show a necessary and sufficient condition for the existence of the tessellation in terms of the moments of the radius distribution. Then we present general expressions for the intensities and the mean k-content of the k-faces of the tessellation. The proofs of these results are rather technical and therefore deferred to Appendix B. In Section 5 some limit results studying the convergence of Laguerre tessellations to Voronoi tessellations are presented. Finally, the obtained general expressions are illustrated for the planar case in Section 6. The formulae are specified, numerically evaluated for some examples, and further results are obtained. In particular, it is possible to explicitly evaluate the probability of a cell being empty. The paper concludes with appendices containing the proofs.

2. Preliminaries

2.1. Basic notation

Throughout this paper, we work in d-dimensional Euclidean space $\mathbb{R}^d$ equipped with the Euclidean norm $\|\cdot\|$ and the corresponding scalar product $\langle\cdot,\cdot\rangle$. For $x \in \mathbb{R}^d$ and $r \geq 0$, let $b(x, r)$ denote the closed d-dimensional ball of radius r centred in x and let $s(x, r) = \partial b(x, r)$ denote the sphere given by its boundary. The d-dimensional unit sphere is denoted by $\mathbb{S}^{d-1}$. Write $\mathcal{B}^d$ for the Borel sets in $\mathbb{R}^d$, λ_d for the d-dimensional Lebesgue measure, and σ for the surface measure on $\mathbb{S}^{d-1}$. Let $\omega_d = \lambda_d(b(0, 1))$ denote the volume, and let $\sigma_d = \sigma(\mathbb{S}^{d-1})$ denote the surface area of the unit ball in $\mathbb{R}^d$, i.e.

$$\omega_d = \frac{\pi^{d/2}}{\Gamma(d/2+1)} \quad \text{and} \quad \sigma_d = 2\frac{\pi^{d/2}}{\Gamma(d/2)}.$$

Let $\mathcal{L}_k^d$ and $\mathcal{E}_k^d$ denote the set of k-dimensional linear and affine subspaces, respectively, of $\mathbb{R}^d$. Write SO_d for the group of rotations about the origin in $\mathbb{R}^d$ and write ν for its unique rotational invariant probability measure. The translation $x + B$ of a set $B \subset \mathbb{R}^d$ by a point $x \in \mathbb{R}^d$ is defined via $x + B = \{x + b : b \in B\}$. The rotation ϑB of B by $\vartheta \in SO_d$ is defined analogously. For $k \in \{0, \dots, d\}$, denote the k-dimensional Hausdorff measure by $\mathcal{H}^k$. Finally, we denote the indicator function of a set $B \subset \mathbb{R}^d$ by $\mathbf{1}_B$, i.e. $\mathbf{1}_B(x) = 1$ if $x \in B$ and $\mathbf{1}_B(x) = 0$ otherwise.

2.2. Tessellations of $\mathbb{R}^d$

A *tessellation* of $\mathbb{R}^d$ is a countable set $T = \{C_i : i \in \mathbb{N}\}$ of sets $C_i \subset \mathbb{R}^d$ (the *cells* of the tessellation) such that

(i) $\operatorname{int}(C_i) \cap \operatorname{int}(C_j) = \varnothing$, $i \neq j$;

(ii) $\bigcup_{i\in\mathbb{N}} C_i = \mathbb{R}^d$;

(iii) T is locally finite, i.e. $\#\{i \in \mathbb{N} : C_i \cap B \neq \varnothing\} < \infty$ for all bounded $B \subset \mathbb{R}^d$; and

(iv) each cell of the tessellation is a compact set with interior points.

If, in addition, all the cells are convex, as it will always be in this paper, then [24, Lemma 6.1.1] implies that the cells are bounded d-dimensional polytopes.

The *faces* of a convex polytope P are the intersections of P with its supporting hyperplanes [22, Section 2.4]. We call a face of P of dimension s, $s \in \{0, \dots, d-1\}$, an *s-face* of P. For convenience, the polytope P itself is considered as a d-face. Write $\mathcal{F}_s(P)$ for the set of s-faces of a polytope P and $\mathcal{F}_s(T) = \bigcup_{i\in\mathbb{N}} \mathcal{F}_s(C_i)$ for the set of s-faces of all cells of the tessellation T.

Furthermore, let $F(y)$ be the intersection of all cells of the tessellation containing the point y. Then $F(y)$ is a finite intersection of d-polytopes and, since it is nonempty, $F(y)$ is an s-dimensional polytope for some $s \in \{0, \dots, d\}$. Therefore, we may introduce

$$\mathcal{S}_s(T) = \{F(y)\colon \dim F(y) = s, y \in \mathbb{R}^d\}, \qquad s = 0, \dots, d,$$

the set of s-faces of the tessellation T. Then an s-face $H \in \mathcal{F}_s(C)$ of a cell C of T is the union of all those s-faces $F \in \mathcal{S}_s(T)$ of the tessellation contained in H.

A tessellation T is called *face-to-face* if the faces of the cells and the faces of the tessellation coincide, i.e. if $\mathcal{S}_s(T) = \mathcal{F}_s(T)$ for $s = 0, \dots, d$. For $s = 0$ and $s = d$, this is always true.

A tessellation T is called *normal* if it is face-to-face and every s-face of T is contained in the boundary of exactly $d - s + 1$ cells for $s = 0, \dots, d - 1$.

Write $\mathbb{T}$ for the set of all tessellations in $\mathbb{R}^d$ and equip it with a suitable σ-field $\mathcal{T}$ as described in [16, p. 46]. A *random tessellation* in $\mathbb{R}^d$ is then a random element X on a probability space $(\Omega, \mathcal{A}, \mathrm{P})$ with range $(\mathbb{T}, \mathcal{T})$. It is called normal or face-to-face if its realisations are almost surely normal or face-to-face, respectively.

The structure of a random tessellation is usually described by means of geometric and topological characteristics of its k-faces. For stationary tessellations, the easiest such characteristics are the intensities of the k-faces, i.e. the mean number of k-faces per unit volume. In order to formalise this, we first define the notion of the centroid of a k-face.

Denote by $\mathcal{P}_k$ the set of k-dimensional polytopes in $\mathbb{R}^d$, and let $c_k\colon \mathcal{P}_k \times \mathbb{T} \to \mathbb{R}^d$ be a measurable *centroid function*, i.e.

$$c_k(F + x, T + x) = c_k(F, T) + x, \qquad x \in \mathbb{R}^d, F \in \mathcal{P}_k, T \in \mathbb{T}, \tag{2.1}$$

such that $c_k(F) \neq c_k(F')$ for different k-faces $F, F' \in \mathcal{S}_k(T)$. We call the point $c_k(F, T)$ the *centroid* of the k-face $F \in \mathcal{S}_k(T)$. For a random tessellation X, we can now introduce the point process N_k of centroids of the k-faces of X. By (2.1), N_k is almost surely a simple and stationary point process whose intensity γ_k is then given by

$$\gamma_k = \mathrm{E}\bigg[\sum_{F \in \mathcal{S}_k(X)} \mathbf{1}_{[0,1]^d}(c_k(F, X))\bigg], \qquad k = 0, \dots, d.$$

The values of γ_k do not depend on the choice of the centroid function c_k [16, p. 47].

Provided that the intensities above are finite, the Palm distribution P_k^0 of N_k can be defined. Under P_k^0, there is a k-face $C_k(0)$ with centroid in the origin. Its distribution is called the distribution of the *typical k-face* of the tessellation X.

Further random measures induced by a random tessellation are the measures

$$M_k(B) = \sum_{F \in \mathcal{S}_k(X)} \mathcal{H}^k(F \cap B), \qquad k = 0, \dots, d,\ B \in \mathcal{B}^d.$$

Their intensities

$$\mu_k = \mathrm{E}\bigg[\sum_{F \in \mathcal{S}_k(X)} \mathcal{H}^k(F \cap [0, 1]^d)\bigg], \qquad k = 0, \dots, d,$$

can be interpreted as the mean total k-content of the k-faces of the tessellation per unit volume. Also, the Palm probability measure Q_k^0 of M_k is of special interest. With respect to this measure, the origin is almost surely contained in a k-face $F_k(0)$ of X.

https://doi.org/10.1239/aap/1222868179 Published online by Cambridge University Press

The Palm measures P_k^0 and Q_k^0 are closely related. In particular, their intensities satisfy

$$\gamma_k = \mu_k \, E_{M_k}^0[\mathcal{H}^k(F_k(0))^{-1}], \tag{2.2}$$

where $E_{M_k}^0$ denotes the expectation with respect to Q_k^0.

As shown in [13], the mean values of the cell characteristics of a planar face-to-face tessellation are completely determined by the values of μ_0 and μ_1 (usually denoted by L_A). For a spatial tessellation, the required parameters are μ_0, μ_1 (L_V), μ_2 (S_V), and the cell intensity, γ_3.

3. Laguerre tessellations

For $y, x \in \mathbb{R}^d$ and $r \geq 0$, define the *power* of y with respect to the sphere $s(x, r)$ as

$$\text{pow}(y, s(x, r)) = \|y - x\|^2 - r^2.$$

Let $\varphi \subset \mathbb{R}^d \times \mathbb{R}_+$ be an at most countable set such that $\min_{(x,r)\in\varphi} \text{pow}(y, s(x, r))$ exists for each $y \in \mathbb{R}^d$. Then the *Laguerre cell* of $(x, r) \in \varphi$ is defined as

$$C((x, r), \varphi) = \{y \in \mathbb{R}^d : \ \text{pow}(y, s(x, r)) \leq \text{pow}(y, s(x', r')), \ (x', r') \in \varphi\}.$$

The point x is called the *nucleus* of the cell $C((x, r), \varphi)$, and the *Laguerre diagram* $L(\varphi)$ is the set of the nonempty Laguerre cells of φ. If the radii of all spheres in φ are equal then $L(\varphi)$ is the Voronoi tessellation of the set $\{x : \ (x, r) \in \varphi\}$.

We will often identify a pair $(x, r) \in \mathbb{R}^d \times \mathbb{R}_+$ with the sphere $s(x, r)$ and use both forms of notation synonymously. Also, the abbreviation $s_i = s(x_i, r_i)$ will be used.

Note that a Laguerre cell does not necessarily contain its nucleus and that a nucleus does not necessarily generate a cell. A necessary condition for a cell to be empty is that the generating sphere is completely contained in the union of the remaining spheres. However, this is not a sufficient condition, as Figure 1 shows.

Given two spheres $s_1 = s(x_1, r_1)$ and $s_2 = s(x_2, r_2)$ in $\mathbb{R}^d$, the points $z \in \mathbb{R}^d$ satisfying $\text{pow}(z, s_1) = \text{pow}(z, s_2)$ form a hyperplane $\text{Ra}(s_1, s_2)$ given by

$$\text{Ra}(s_1, s_2) = \{z \in \mathbb{R}^d : 2\langle z, x_1 - x_2\rangle = \|x_1\|^2 - \|x_2\|^2 + r_2^2 - r_1^2\},$$

which is perpendicular to the line joining x_1 and x_2 and called the *radical axis* of s_1 and s_2. If two spheres intersect then their radical axis passes through their intersections. If two spheres have equal radii, their radical axis is the perpendicular bisector of the line joining their centres.

Every s-face $F \in \mathcal{S}_s(L(\varphi))$ can be written as

$$F = F(s_0, \ldots, s_k, \varphi) = \bigcap_{i=0}^{k} C(s_i, \varphi), \qquad s_0, \ldots, s_k \in \varphi, \tag{3.1}$$

with a suitable number of cells involved. Then $F(s_0, \ldots, s_k, \varphi)$ is included in the affine subspace $\{y \in \mathbb{R}^d : \ \text{pow}(y, s_0) = \cdots = \text{pow}(y, s_k)\}$.

For $\varphi \subset \mathbb{R}^d \times \mathbb{R}_+$, introduce the following regularity conditions:

(R1) for every $y \in \mathbb{R}^d$ and every $t \in \mathbb{R}$, only finitely many elements $(x, r) \in \varphi$ satisfy $\|y - x\|^2 - r^2 \leq t$; and

(R2) the convex hull of $\{x : \ (x, r) \in \varphi\}$ is the whole space $\mathbb{R}^d$.

https://doi.org/10.1239/aap/1222868179 Published online by Cambridge University Press

If the set of radii is bounded, condition (R1) implies the local finiteness of the set of points $\{x : (x, r) \in \varphi\}$.

Furthermore, we say that the points of φ are in *general position* if

(GP1) no $k + 1$ nuclei are contained in a $(k - 1)$-dimensional affine subspace of $\mathbb{R}^d$ for $k = 2, \dots, d$; and

(GP2) no $d + 2$ points have equal power with respect to some point in $\mathbb{R}^d$.

In the case of equal radii this is exactly the property addressed as general quadratic position in [18, p. 5].

Theorem 3.1. *If the set $\varphi \subset \mathbb{R}^d \times \mathbb{R}_+$ satisfies the regularity conditions (R1) and (R2) then the set of the Laguerre cells $C((x, r), \varphi)$, $(x, r) \in \varphi$, with nonvanishing interior is a face-to-face tessellation of $\mathbb{R}^d$. If, in addition, the points of φ are in general position then all the cells of $L(\varphi)$ have dimension d and the Laguerre tessellation $L(\varphi)$ is normal.*

For the proof, we refer the reader to [12] and [21].

Aurenhammer [2] gave a complete characterisation of the set of Laguerre diagrams generated by finite sets of spheres. A very pleasing result is that each finite normal cell complex can be realised as a Laguerre diagram. However, diagrams with finitely many cells necessarily contain unbounded cells; hence, they do not belong to $\mathbb{T}$. Theorem 3.2, below, generalises Aurenhammer's results to the case of infinitely many spheres (or cells), which then also applies to tessellations in the sense defined above. The proof can be found in Appendix A.

Theorem 3.2. *Every normal tessellation of $\mathbb{R}^d$ with convex cells for $d \geq 3$ is a Laguerre tessellation.*

Note that the above statement cannot be strengthened to include $d = 2$, a counterexample is given in [2].

4. Poisson–Laguerre tessellations

From now on we will assume that the set φ is a realisation of a stationary, independently marked Poisson process Φ on $\mathbb{R}^d \times \mathbb{R}_+$ with intensity $\lambda > 0$ and mark distribution ρ. The proofs of the statements in this section are mainly given in Appendix B.

Theorem 4.1. *Suppose that R is a positive random variable with distribution ρ. Then the Laguerre tessellation of Φ exists, i.e. $\min_{(x,r)\in\Phi} \operatorname{pow}(y, (x, r)) > -\infty$ almost surely for all $y \in \mathbb{R}^d$, if and only if $\mathrm{E}[(R \vee 1)^d] < \infty$, where $a \vee b = \max(a, b)$.*

From now on we will assume that the mark distribution ρ of Φ satisfies the condition $\mathrm{E}[(R \vee 1)^d] < \infty$.

Theorem 4.2. *The Laguerre tessellation of Φ is a normal random tessellation.*

Now we pass to the properties related to the Palm probability measure Q_k^0 defined in Section 2. Its complete description in terms of integrals has been obtained in [12], the special case of the Voronoi tessellation has been studied in [5]. Here, we only state the formulae for the mean number γ_k and the mean k-content μ_k of k-faces per unit volume.

https://doi.org/10.1239/aap/1222868179 Published online by Cambridge University Press

For a natural number m and $x_0, \dots, x_m \in \mathbb{R}^m$, let $\Delta_m(x_0, \dots, x_m)$ be the m-dimensional volume of the convex hull of $x_0, \dots, x_m$ in $\mathbb{R}^m$. For $w_0, \dots, w_m \geq 0$, define

$$V_{m,k}(w_0, \dots, w_m) = (m!)^{k+1} \int_{\mathbb{S}^{m-1}} \cdots \int_{\mathbb{S}^{m-1}} \Delta_m^{k+1}(w_0 u_0, \dots, w_m u_m) \sigma(\mathrm{d}u_0) \cdots \sigma(\mathrm{d}u_m).$$

In the remainder of this section,

$$p(t) = \exp\biggl(-\lambda \omega_d \int_0^\infty ([t + r^2]^+)^{d/2} \rho(\mathrm{d}r)\biggr),$$

where $t^+ = \max(t, 0)$, is the probability that the power from the origin to each point of Φ exceeds t; see (B.1) in Appendix B.

Theorem 4.3. *Let Φ be a stationary marked Poisson process with intensity $\lambda > 0$ and mark distribution ρ satisfying $\mathrm{E}[(R \vee 1)^d] < \infty$. The intensities $\mu_k, 0 < k < d$, are given by the formula*

$$\begin{aligned}\mu_k = {} & \frac{\lambda^{m+1}}{4(m+1)!} c_{dm} \sigma_k \\ & \times \int_0^\infty \cdots \int_0^\infty \int_{-\min_i r_i^2}^\infty \prod_{i=0}^m (t + r_i^2)^{(m-2)/2} V_{m,k}((t + r_0^2)^{1/2}, \dots, (t + r_m^2)^{1/2}) \\ & \times \int_0^\infty p(s + t) s^{(k-2)/2} \, \mathrm{d}s \, \mathrm{d}t \rho(\mathrm{d}r_0) \cdots \rho(\mathrm{d}r_m), \end{aligned} \qquad (4.1)$$

where $m = d - k$ and $c_{dm} = \sigma_{d-m+1} \cdots \sigma_d / \sigma_1 \cdots \sigma_m$. For $k = d$, we have $\mu_d = 1$, for $k = 0$,

$$\begin{aligned}\mu_0 = {} & \frac{\lambda^{d+1}}{2(d+1)!} \\ & \times \int_0^\infty \cdots \int_0^\infty \int_{-\min_i r_i^2}^\infty \prod_{i=0}^d (t + r_i^2)^{(d-2)/2} V_{d,0}((t + r_0^2)^{1/2}, \dots, (t + r_d^2)^{1/2}) \\ & \times p(t) \, \mathrm{d}t \rho(\mathrm{d}r_0) \cdots \rho(\mathrm{d}r_d). \end{aligned}$$

The formulae for μ_k cannot be evaluated further because of the lack of an explicit formula for $V_{m,k}(w_0, \dots, w_m)$. However, a formula by Miles [14] shows that

$$V_{m,k}(1, \dots, 1) = 2^{m+1} \pi^{m(m+1)/2} \frac{\Gamma((1/2)(m+1)(d+1) - m)}{\Gamma(md/2)\Gamma((d+1)/2)^{m+1}} \prod_{i=1}^m \frac{\Gamma((1/2)(k+1+i))}{\Gamma(i/2)}. \qquad (4.2)$$

For a degenerate radius distribution ρ, i.e. the case of a Poisson–Voronoi tessellation, applying (4.2) to (4.1) leads to the well-known values

$$\mu_k^V = \frac{\lambda^{m/d} 2^{m+1} \pi^{m/2} \Gamma((dm + k + 1)/2) \Gamma(d/2 + 1)^{m+k/d} \Gamma(m + k/d)}{d(m+1)! \, \Gamma((dm + k)/2) \Gamma((d+1)/2)^m \Gamma((k+1)/2)}.$$

While this formula is explicit, the computation of μ_k for other radius distributions ρ usually requires numerical integration. Some examples will be considered in Section 6.

Nevertheless, it can indeed be shown that the intensities μ_k, $k = 0, \dots, d$, are finite [12, Theorem 3.2.9]. Hence, the Palm probability measure Q_k^0 is well defined.

Relation (2.2) can be used to obtain formulae for the intensities γ_k. However, in contrast to the formulae for μ_k, they appear intractable to the application of numerical methods.

Theorem 4.4. *For $0 < k < d$, the intensity γ_k of the k-faces is given by*

$$\begin{aligned}\gamma_k = {} & \frac{\lambda^{m+1}}{4(m+1)!} c_{dm} \sigma_k \\ & \times \int_0^\infty \cdots \int_0^\infty \int_{-\min_i r_i^2}^\infty \prod_{i=0}^m (t + r_i^2)^{(m-2)/2} V_{m,k}((t + r_0^2)^{1/2}, \dots, (t + r_m^2)^{1/2}) \\ & \times \int_0^\infty p(t+s) s^{(k-2)/2} \, \mathrm{E}[A_{L^\perp}(t, s, \Phi^{s+t})^{-1}] \, \mathrm{d}s \, \mathrm{d}t \rho(\mathrm{d}r_0) \cdots \rho(\mathrm{d}r_m),\end{aligned}$$

where $L \in \mathcal{L}_m^d$ is a fixed subspace of $\mathbb{R}^d$, $\Phi^t = \Phi \cap \{(x, r) \colon \operatorname{pow}(0, (x, r)) > t\}$,

$$A_{L^\perp}(t, s, \eta) = \int_0^\infty l^{k-1} \int_{\mathbb{S}^{d-1} \cap L^\perp} \mathbf{1}\{\tau(l, t, s, v, u) \le \operatorname{pow}(lv, (x, r)),\ (x, r) \in \eta\} \sigma_{L^\perp}(\mathrm{d}v) \, \mathrm{d}l$$

with $\tau(l, t, s, u, v) = l^2 + t + s - 2ls^{1/2}\langle u, v\rangle$ for fixed $u \in \mathbb{S}^{d-1} \cap L^\perp$, and $\sigma_{L^\perp}$ is the surface measure on the $(d-m)$-dimensional sphere $\mathbb{S}^{d-1} \cap L^\perp$.

The formula for the cell intensity γ_d reads

$$\gamma_d = \frac{\lambda \sigma_d}{2} \int_0^\infty \int_{-r_0^2}^\infty (t + r_0^2)^{(d-2)/2} p(t) \, \mathrm{E}[A(t, r_0, u, \Phi^t)^{-1}] \, \mathrm{d}t \rho(\mathrm{d}r_0),$$

where $u \in \mathbb{S}^{d-1}$ is fixed and

$$A(t, r_0, u, \eta) = \int_0^\infty l^{d-1} \int_{\mathbb{S}^{d-1}} \mathbf{1}\{\zeta(l, t, r_0, v, u) \le \operatorname{pow}(lv, (x, r)),\ (x, r) \in \eta\} \sigma(\mathrm{d}v) \, \mathrm{d}l$$

with $\zeta(l, t, r_0, u, v) = l^2 + t - 2l([t + r_0^2]^+)^{1/2}\langle u, v\rangle$.

4.1. Typical faces

In Section 2 we defined two Palm measures P_k^0 and Q_k^0. Under P_k^0, there is a k-face $C_k(0)$ with centroid in the origin, allowing us to call this random element a typical k-face. In contrast, with respect to Q_k^0, the origin has been 'uniformly' chosen on the k-dimensional boundary of the tessellation which gives rise to a k-face $F_k(0)$ containing the origin. Then $F_k(0)$ is, in a sense, a typical edge weighted with its k-content. In particular, $F_d(0)$ is simply the cell containing the origin. In the following, we will give the formulae for the mean k-content of the k-faces $F_k(0)$ and $C_k(0)$.

Denote by $\kappa(l, r_1, r_2)$ the volume of the union of two balls with radii r_1 and r_2 and centres separated by distance l. There is an explicit expression for this union, which is rather cumbersome; see, e.g. [12, Proposition 3.3.4]. Introduce, for $l \ge 0$ and $t_1, t_2 \in \mathbb{R}$,

$$\xi(l, t_1, t_2) = \exp\biggl(-\lambda \int_0^\infty \kappa(l, ([t_1 + r^2]^+)^{1/2}, ([t_2 + r^2]^+)^{1/2}) \rho(\mathrm{d}r)\biggr). \tag{4.3}$$

https://doi.org/10.1239/aap/1222868179 Published online by Cambridge University Press

Theorem 4.5. *The mean k-content of the k-dimensional face $F_k(0)$ for $0 < k < d$ is given by*

$$\begin{aligned}\mu_k \, \mathrm{E}^0_{M_k}[\mathcal{H}^k(F_k(0))] &= \frac{\lambda^{m+1}}{4(m+1)!} c_{dm} \sigma_k \\ &\quad \times \int_0^\infty \cdots \int_0^\infty \int_{-\min_i r_i^2}^\infty \prod_{i=0}^m (t + r_i^2)^{(m-2)/2} V_{m,k}((t+r_0^2)^{1/2}, \ldots, (t+r_m^2)^{1/2}) \\ &\quad \times \int_0^\infty s^{(k-2)/2} \int_0^\infty l^{k-1} \int_{S^{d-1} \cap L^\perp} \xi(l, s+t, \tau(l,t,s,u,v)) \\ &\qquad\qquad \times \sigma(\mathrm{d}v)\,\mathrm{d}l\,\mathrm{d}s\,\mathrm{d}t \rho(\mathrm{d}r_0) \cdots \rho(\mathrm{d}r_m),\end{aligned}$$

where $u \in \mathbb{S}^{d-1} \cap L^\perp$ is a fixed vector and the function ξ is defined in (4.3). For the mean volume of $F_d(0)$, we have

$$\begin{aligned}&\mathrm{E}^0_{M_d}[\mathcal{H}^d(F_d(0))] \\ &\quad = \frac{\lambda \sigma_d}{2} \int_0^\infty \int_{-r_0^2}^\infty (t + r_0^2)^{(d-2)/2} \int_0^\infty l^{d-1} \int_{S^{d-1}} \xi(l, t, \rho(l, t, r_0, u, v)) \sigma(\mathrm{d}v)\,\mathrm{d}l\,\mathrm{d}t \rho(\mathrm{d}r_0).\end{aligned}$$

A formula for the mean k-content of the typical k-face $C_k(0)$ is obtained from the previous results via the relation $\gamma_k E^0_{N_k}[\mathcal{H}^k(C_k(0))] = \mu_k$. Further formulae for distributions related to the typical k-faces $F_k(0)$ and $C_k(0)$, in particular the joint distribution of their generators, are given in [12, Section 3.3].

4.2. Contact distributions

Recall that, for a random closed set X and a convex compact set B in $\mathbb{R}^d$ containing the origin, the *contact distribution function* H_B is defined via

$$H_B(r) = \mathrm{P}(X \cap rB \neq \varnothing \mid 0 \notin X), \qquad r \geq 0.$$

The random closed set of interest here is the union of cell boundaries of the tessellation. Since the origin is almost surely contained in the cell $F_d(0)$, we have $H_B(r) = 1 - \mathrm{P}(rB \subset F_d(0))$ for every choice of B. Important special cases are the *spherical contact distribution function* H_s, where $B = b(0, 1)$ is the unit ball centred in the origin, and the *linear contact distribution function* $H_{l(v)}$, where $B = l(v)$ is a line segment of unit length in direction $v \in S^{d-1}$.

Contact and chord length distributions of the Poisson–Voronoi tessellation have been studied in [19], while the Voronoi tessellation with respect to more general point processes has been investigated in [10]. For Poisson–Laguerre tessellations, we have the following result.

Theorem 4.6. *The linear contact distribution function $H_{l(v)}$ for $v \in S^{d-1}$ is given by*

$$\begin{aligned}1 - H_{l(v)}(r) &= \frac{\lambda}{2} \int_0^\infty \int_{-r_0^2}^\infty (t + r_0^2)^{(d-2)/2} \\ &\qquad \times \int_{S^{d-1}} \xi(r, t, \rho(r, t, r_0, u, v)) \sigma(\mathrm{d}u)\,\mathrm{d}t \rho(\mathrm{d}r_0), \qquad r \geq 0,\end{aligned}$$

where $\xi(l, t_1, t_2)$ is defined in (4.3).

https://doi.org/10.1239/aap/1222868179 Published online by Cambridge University Press

Since the Poisson–Laguerre tessellation is isotropic, the values of $H_{l(v)}(r)$ do not depend on the direction v of the line segment.

An expression for the spherical contact distribution function can also be obtained and is given in [12, Corollary 3.3.16].

5. Limit results

Since a Voronoi tessellation can be interpreted as a Laguerre tessellation with respect to a degenerate distribution of radii, it is natural to consider Poisson–Voronoi tessellations as limits of Poisson–Laguerre tessellations when changing the parameters of the mark distribution. In this section we present some limit results which we prove in Appendix B.

Consider a stationary marked Poisson process Φ on $\mathbb{R}^d \times \mathbb{R}_+$ with intensity λ and mark distribution ρ satisfying $\mathrm{E}[(R \vee 1)^d] < \infty$. Write $\Phi_v = \{(x, vr) : (x, v) \in \Phi\}$, $v > 0$, for a mark-scaled version of the point process Φ.

The first result states that a Laguerre tessellation converges to a Voronoi tessellation if the radii are reduced to 0. Recall that a closed set F_n converges to F in Wijsman topology if the distance functions $d(x, F_n) = \inf_{y \in F_n} \|x - y\|$ converge to $d(x, F)$ for every x; see, e.g. [15, p. 401].

Theorem 5.1. *Almost surely, as $v \downarrow 0$, the boundary $\mathcal{F}_{d-1}(L(\Phi_v))$ of the Laguerre tessellation $L(\Phi_v)$ converges in Wijsman topology to the boundary $\mathcal{F}_{d-1}(L^V(\hat{\Phi}))$ of the Voronoi tessellation $L^V(\hat{\Phi})$ constructed with respect to the Poisson process $\hat{\Phi} = \{x \in \mathbb{R}^d : (x, v) \in \Phi\}$ with intensity λ.*

The next limiting regime is when there is an atom at the maximum value of the radius distribution, implying that the corresponding largest radius cells will eventually dominate the others.

Theorem 5.2. *Assume that the mark distribution ρ is supported by a bounded segment $[0, s]$ and is such that $\rho(\{s\}) = p > 0$. Denote by $\tilde{\Phi} = \{x \in \mathbb{R}^d : (x, s) \in \Phi\}$ the subset of points carrying the weight s (which is a Poisson process with intensity $p\lambda$ in $\mathbb{R}^d$). Then almost surely for any bounded set $W \subset \mathbb{R}^d$ there exists $v_0 = v_0(\Phi, W) > 0$ such that the boundary of the Laguerre tessellation $L(\Phi_v)$ inside W coincides with the boundary of the Voronoi tessellation $L^V(\tilde{\Phi})$ restricted to W for all $v > v_0$.*

This theorem also implies the almost sure Wijsman convergence of the boundaries $\mathcal{F}_{d-1}(L(\Phi_v))$ to their Voronoi tessellation counterparts. But the result formulated above is stronger, of 'a finite coupling time' type.

Convergence in the above schemes is also discussed in [12] in terms of the Palm distributions P_k^0 corresponding to the k-faces of the tessellation.

6. The planar case

For applications, the cases in which $d = 2$ and $d = 3$ are of special interest. In this section we discuss the planar case in detail: more explicit formulae for μ_0 and μ_1 are obtained and evaluated for some examples. Furthermore, we derive a formula for the probability p_0 that the typical point of Φ generates a nonempty cell.

The main problem when working with the expressions in Theorem 4.3 is the lack of explicit general formulae for $\Delta_m^{k+1}(w_0u_0, \dots, w_mu_m)$ and $V_{m,k}(w_0, \dots, w_m)$. However, in some special cases it is possible to overcome this problem. In the two-dimensional case we have to

https://doi.org/10.1239/aap/1222868179 Published online by Cambridge University Press

consider Δ_2 and Δ_1^2. Unfortunately, $\Delta_2(w_0u_0, w_1u_1, w_2u_2)$ remains intractable. But we have

$$\Delta_1^2(w_0u_0, w_1u_1) = w_0^2 + w_1^2 - 2\langle u_0, u_1\rangle w_0 w_1, \qquad u_0, u_1 \in \mathbb{S}^1 \cap L,\ w_0, w_1 > 0,$$

and, therefore, $V_{1,1}(w_0, w_1) = 4(w_0^2 + w_1^2)$.

For the intensities μ_0 and μ_1, we obtain

$$\mu_0 = \frac{\lambda^3}{12} \iiint_{\mathbb{R}_+^3} \int_{-\min_i r_i^2}^{\infty} \exp\biggl(-\lambda\pi \int_0^\infty [t + r^2]^+ \rho(\mathrm{d}r)\biggr) \times V_{2,0}((t + r_0^2)^{1/2}, (t + r_1^2)^{1/2}(t + r_2^2)^{1/2})\, \mathrm{d}t\rho(\mathrm{d}r_0)\rho(\mathrm{d}r_1)\rho(\mathrm{d}r_2)$$

and

$$\mu_1 = \lambda^2\pi \iint_{\mathbb{R}_+^2} \int_{-\min_i r_i^2}^{\infty} \frac{2t + r_0^2 + r_1^2}{(t + r_0^2)^{1/2}(t + r_1^2)^{1/2}} \times \int_0^\infty \exp\biggl(-\lambda\pi \int_0^\infty [t + s + r^2]^+ \rho(\mathrm{d}r)\biggr) \times s^{-1/2}\, \mathrm{d}s\, \mathrm{d}t\rho(\mathrm{d}r_0)\rho(\mathrm{d}r_1).$$

These two formulae provide all the parameters which are required for computing the mean values of the cell characteristics using the mean-value relations for normal tessellations [13]. In particular, we can derive a formula for the probability p_0 that the typical point of Φ generates a nonempty cell: since the intensity of cells is given by $\gamma_2 = p_0\lambda$ and $\mu_0 = \gamma_0 = 2\gamma_2$, we have

$$p_0 = \frac{\lambda^2}{24} \iiint_{\mathbb{R}_+^3} \int_{-\min_i r_i^2}^{\infty} \exp\biggl(-\lambda\pi \int_0^\infty [t + r^2]^+ \rho(\mathrm{d}r)\biggr) \times V_{2,0}((t + r_0^2)^{1/2}, (t + r_1^2)^{1/2}, (t + r_2^2)^{1/2}) \times \mathrm{d}t\rho(\mathrm{d}r_0)\rho(\mathrm{d}r_1)\rho(\mathrm{d}r_2).$$

As an example, we consider the Poisson–Laguerre tessellation for the case where ρ is a two-atom distribution, taking the value a with probability q and the value $b > a$ with probability $1-q$. The parameters are chosen as $\lambda = 100$, $a = 0.01$, $b = 0.01, 0.05, 0.10, 0.15, 0.20, 0.25, 0.30$, and $q = 0.5$. This means that we start with a Poisson–Voronoi tessellation of intensity $\lambda = 100$ and gradually increase the value of the larger radius.

The formulae for $\mu_0(= \gamma_0)$ and $\mu_1(= L_A)$ are evaluated using the numerical integration functions of MATHEMATICA®. From these, the mean values of characteristics of the typical nonempty cell are computed using the mean-value relations. The results are summarised in Table 1. For comparison, the values for Poisson–Voronoi tessellations with intensities $\lambda = 100$ and $\lambda = 50$ are included.

When investigating the intensities μ_k of the measures M_k, we may ask not only for the total value of μ_k but also for the contribution of each class of k-faces to this value. Hence, we write $\mu_0(r_0, r_1, r_2)$ for the intensity of vertices whose neighbours carry the weights r_0, r_1, and r_2 and $\mu_1(r_0, r_1)$ for the total length of edges whose neighbours carry the weights r_0 and r_1. Clearly,

$$\mu_0 = \mu_0(a, a, a) + \mu_0(a, a, b) + \mu_0(a, b, b) + \mu_0(b, b, b),$$
$$\mu_1 = \mu_1(a, a) + \mu_1(a, b) + \mu_1(b, b).$$

The results of the numerical evaluation for the example discussed above are presented in Table 2.

https://doi.org/10.1239/aap/1222868179 Published online by Cambridge University Press

TABLE 1: Mean values of cell characteristics for a two-dimensional Laguerre tessellation generated by a stationary Poisson process of intensity $\lambda = 100$ with marks independently drawn from a two-atom distribution taking the values 0.01 and b with probability 0.5 each. The columns PV_{100} and PV_{50} contain the values for Poisson–Voronoi tessellations with intensities $\lambda = 100$ and $\lambda = 50$, respectively. Given are the intensities of the k-faces γ_k, the mean total edge length per unit volume L_A, the mean length l_1 of the typical edge, and the mean area a_2 and the perimeter u_2 of the typical cell.

b	PV_{100}	0.05	0.10	0.15	0.20	0.25	0.30	PV_{50}
γ_0	200.000	192.406	148.398	110.968	101.050	100.043	100.001	100.000
γ_1	300.000	288.609	222.597	166.452	151.574	150.065	150.001	150.000
γ_2	100.000	96.203	74.199	55.484	50.525	50.022	50.001	50.000
L_A	20.000	19.203	16.283	14.529	14.173	14.143	14.142	14.142
l_1	0.067	0.066	0.073	0.087	0.094	0.094	0.094	0.094
a_2	0.010	0.010	0.014	0.018	0.020	0.020	0.020	0.020
u_2	0.400	0.399	0.439	0.524	0.561	0.566	0.566	0.566

TABLE 2: Contributions of different cell types to μ_0 and μ_1.

b	PV_{100}	0.05	0.10	0.15	0.20	0.25	0.30	PV_{50}
$\mu_0(b,b,b)$	25.000	35.627	67.743	92.562	99.263	99.969	99.999	100.000
$\mu_0(a,b,b)$	75.000	77.291	48.678	12.652	1.331	0.058	0.001	0.000
$\mu_0(a,a,b)$	75.000	62.341	26.699	5.013	0.408	0.015	0.000	0.000
$\mu_0(a,a,a)$	25.000	17.148	5.279	0.741	0.047	0.001	0.000	0.000
$\mu_1(b,b)$	5.000	6.935	11.239	13.615	14.100	14.141	14.142	14.142
$\mu_1(a,b)$	10.000	8.839	3.987	0.766	0.063	0.002	0.000	0.000
$\mu_1(a,a)$	5.000	3.430	1.056	0.148	0.010	0.000	0.000	0.000

Convergence to a Poisson–Voronoi tessellation of intensity $\lambda = 50$ with increasing b in line with Theorem 5.2 is clearly visible in both tables. It turns out that already for $b = 0.3$ nearly all of the cells generated by points with the smaller weight have disappeared.

A number of further numeric results can be found in [12]. These include numerical evaluations of the formulae presented here for the case of a uniform distribution of radii. Distributions of cell characteristics, namely the probability density functions of the area, perimeter, and number of edges of a typical Poisson–Laguerre cell in $\mathbb{R}^2$ are studied by simulation. In addition, the spatial case, $d = 3$, is discussed in detail.

Appendix A. Proof of Theorem 3.2

In this section we consider the more general situation where the weights of the points do not necessarily have to be positive. Hence, we will work with weights w_i rather than with the radii r_i. Nevertheless, we will use the abbreviation s_i for the pairs (x_i, w_i).

Definition A.1. Consider a tessellation $T = \{C_i : i \in \mathbb{N}\}$ of $\mathbb{R}^d$. An *orthogonal dual* of T is a point set $\mathcal{D}(T) = \{x_i : i \in \mathbb{N}\}$ in $\mathbb{R}^d$ with the following properties.

(i) *Duality.* Each cell C_i of T is associated with exactly one point $x_i \in \mathcal{D}(T)$ such that $x_i \neq x_j$ for $i \neq j$.

https://doi.org/10.1239/aap/1222868179 Published online by Cambridge University Press

(ii) *Orthogonality.* For cells C_i and C_j, $i \neq j$, of T, let $L_{i,j}$ denote the line connecting x_i and x_j. Then $L_{i,j}$ is orthogonal to $C_i \cap C_j$.

(iii) *Orientation.* Any ray parallel to $L_{i,j}$ directed from x_i to x_j and intersecting both of C_i and C_j first meets C_i.

Theorem A.1. *A tessellation T of $\mathbb{R}^d$ is the Laguerre tessellation of some set φ if and only if an orthogonal dual $\mathcal{D}(T)$ of T exists.*

Proof. If T is a Laguerre tessellation of $\mathbb{R}^d$, the set of nuclei yields the required orthogonal dual. Conversely, consider a tessellation $T = \{C_i : i \in \mathbb{N}\}$ of $\mathbb{R}^d$ and assume the existence of an orthogonal dual $\mathcal{D}(T) = \{x_i : i \in \mathbb{N}\}$. Sort the points x_i in increasing distance from the origin, ordering points with equal distance lexicographically. We will now iteratively assign weights w_i to the points x_i such that T is the Laguerre tessellation of the set $\varphi = \{(x_i, w_i) : i \in \mathbb{N}\}$. The weight w_1 can be chosen arbitrarily. Consider three cells C_i, C_j, and C_m, $i < j < m$, such that $F = C_i \cap C_j \cap C_m \neq \varnothing$, and assume that w_i has already been constructed. Denote the closed half-space bounded by $\mathrm{Ra}(s_i, s_j)$ by

$$H(s_i, s_j) = \{z \in \mathbb{R}^d : 2\langle z, x_i - x_j\rangle \geq \|x_i\|^2 - \|x_j\|^2 + w_j - w_i\},$$

and write $s_i \sim s_j$ if $C_i \subseteq H(s_i, s_j)$ and $C_j \subseteq H(s_j, s_i)$. A result in [2, Fact 1] shows that, for any weight w_i of s_i and for any cell C_j distinct from C_i, there exists a w_j such that $s_j \sim s_i$. Hence, we find weights w_j and w_m such that $s_j \sim s_i$ and $s_m \sim s_i$. Then $F \subset \mathrm{Ra}(s_i, s_j) \cap \mathrm{Ra}(s_i, s_m)$. Since the radical axes of s_i, s_j, and s_m are not parallel, they intersect in a common $(d-2)$-dimensional subspace of $\mathbb{R}^d$. Therefore, we also have $F \subset \mathrm{Ra}(s_j, s_m)$. Obviously, $F \subset C_j \cap C_m$. Since both $C_j \cap C_m$ and $\mathrm{Ra}(s_j, s_m)$ are orthogonal to the line joining x_j and x_m and contain F, we conclude that $C_j \cap C_m \subset \mathrm{Ra}(s_j, s_m)$. Furthermore, the orientation of $\mathcal{D}(T)$ yields $C_j \subset H(s_j, s_m)$. This implies transitivity of the relation '$\sim$' for $F \neq \varnothing$, which allows the construction of a set $\varphi = \{s_i : i \in \mathbb{N}\}$ such that $T = L(\varphi)$.

In order to give the proof of Theorem 3.2, we first fix some notation. Let $T = \{C_i : i \in \mathbb{N}\}$ be a normal tessellation of $\mathbb{R}^d$. For $i \geq d$, define $Q_i = \bigcup_{j=1}^{i} C_j$, and let v be a vertex in the boundary of Q_i. Denote by $e_1, \dots, e_s$ the edges in ∂Q_i having v as a vertex. We say that Q_i is *concave* at v if the convex hull of $\{e_1, \dots, e_s\}$ is not contained in Q_i. Since T is normal, concavity of Q_i implies the existence of a unique cell C of T containing all faces F in ∂Q_i with $v \in F$. This cell is called *proper* with respect to Q_i.

Proof of Theorem 3.2. Let T be a normal tessellation of $\mathbb{R}^d$ with $d \geq 3$. We will introduce a certain ordering $C_1, C_2, \dots$ of the cells of T which can then be used for an iterative construction of an orthogonal dual $\mathcal{D}(T) = \{x_1, x_2, \dots\}$.

Choose $C_1, \dots, C_d$ such that they share a common edge. A set of points $x_1, \dots, x_d$ that satisfies duality, orthogonality, and orientation can easily be found. For $i > d$, choose C_i proper with respect to Q_{i-1} such that Q_i is simply connected. For $j < i$, denote by $F_{j,i}$ the face $C_i \cap C_j$ (if it exists) and denote by $L_{j,i}$ the line orthogonal to $F_{j,i}$ through x_j. Define $F_i = Q_{i-1} \cap C_i$. If we show that $x_i = \bigcap_{F_{j,i} \in F_i} L_{j,i}$ is a singleton, this implies orthogonality of the set $X_i = \{x_1, \dots, x_i\}$. Duality and orientation of X_i follow from the convexity of C_i.

Call a vertex in $F_i \setminus \partial Q_i$ an inner vertex of F_i. By [2, Claim 1], for any inner vertex v of F_i, the intersection $\bigcap_{v \in F_{j,i}} L_{j,i}$ is a single point z. If the set of inner vertices of $F_i \setminus \partial Q_i$ contains exactly one element, we set $x_i = z$. Otherwise, let v and v' be two inner vertices joined by the edge e. Then there exist unique points $z = \bigcap_{v \in F_{j,i}} L_{j,i}$ and $z' = \bigcap_{v' \in F_{t,i}} L_{t,i}$. Since, by

https://doi.org/10.1239/aap/1222868179 Published online by Cambridge University Press

[2, Claim 2], the graph consisting of the inner vertices of F_i and the edges joining them is connected, it is sufficient to show that, for any such v and v', the points z and z' coincide. The edge e is contained in exactly $(d-1)$ two-faces of F_i; hence, $j=t$ occurs for $(d-1)$ values of j. Since $d \geq 3$, the intersection point $z=z'$ is uniquely determined by the $(d-1)$ lines corresponding to these indices.

Repeating this construction, the set $\bigcup_i X_i$ yields an orthogonal dual $\mathcal{D}(T)$ of T. Hence, Theorem A.1 shows that T is a Laguerre tessellation.

Appendix B. Proofs from Section 4

Proof of Theorem 4.1. For suitable functions v, the generating functional G of an independently marked Poisson process Φ is given by the formula

$$G(v) = \mathrm{E}\bigg[\prod_{(x,r)\in\Phi} v(x,r)\bigg] = \exp\bigg(-\lambda \int (1-v(x,r))\lambda_d(\mathrm{d}x)\rho(\mathrm{d}r)\bigg).$$

Let $y \in \mathbb{R}^d$ be an arbitrary point, and denote by $p(t)$ the probability that the power from y to each point of Φ exceeds t. Then

$$\begin{aligned} p(t) &= \mathrm{E}\bigg[\prod_{(x,r)\in\Phi} \mathbf{1}\{\mathrm{pow}(y,(x,r)) > t\}\bigg] \\ &= \exp\bigg(-\lambda \int_0^\infty \int_{\mathbb{R}^d} \mathbf{1}\{\mathrm{pow}(y,(x,r)) \leq t\}\lambda_d(\mathrm{d}x)\rho(\mathrm{d}r)\bigg) \\ &= \exp\bigg(-\lambda \int_0^\infty \int_{\mathbb{R}^d} \mathbf{1}\{\|y-x\|^2 \leq t+r^2\}\lambda_d(\mathrm{d}x)\rho(\mathrm{d}r)\bigg) \\ &= \exp\bigg(-\lambda\omega_d \int_0^\infty ([t+r^2]^+)^{d/2}\rho(\mathrm{d}r)\bigg), \end{aligned} \tag{B.1}$$

where $t^+ = \max(t,0)$. If $\mathrm{E}[(R \vee 1)^d] < \infty$ then

$$\begin{aligned} \mathrm{P}\Big(\inf_{(x,r)\in\Phi} \mathrm{pow}(y,(x,r)) = -\infty\Big) &= \lim_{t\to-\infty} \mathrm{P}\Big(\inf_{(x,r)\in\Phi} \mathrm{pow}(y,(x,r)) < t\Big) \\ &= \lim_{t\to-\infty} (1-p(t)) \\ &= 0. \end{aligned}$$

Thus, for each $y \in \mathbb{R}^d$, we have at least one point $(x,r) \in \Phi$ minimising $\mathrm{pow}(y,(x,r))$. Hence, $y \in C((x,r),\Phi)$. On the other hand, $\mathrm{E}[(R\vee 1)^d] = \infty$ implies that $p(t)=0$ for each $t \in \mathbb{R}$ and, therefore, $\inf_{(x,r)\in\Phi} \mathrm{pow}(y,(x,r)) = -\infty$ with probability 1.

Proof of Theorem 4.2. We will check the applicability of Theorem 3.1. The property $\mathrm{pow}(y,(x,r)) \leq t$ for $(x,r)\in\Phi$ is equivalent to $y \in b(x,\sqrt{[t+r^2]^+})$ for $(x,r)\in\Phi$. In other words, y is contained in the Boolean model of balls $b(x,\sqrt{[t+r^2]^+})$ with $(x,r)\in\Phi$. For such a Boolean model, the condition $\mathrm{E}[R^d] < \infty$ implies that, for each bounded set $B \subset \mathbb{R}^d$, the set $\{(x,r)\in\Phi\colon b(x,\sqrt{[t+r^2]^+}) \cap B \neq \varnothing\}$ is almost surely finite. With $B=\{y\}$, this implies condition (R1). Regularity condition (R2) is a consequence of the stationarity of Φ [24, Satz 1.3.5]. The proof that (GP1) and (GP2) are fulfilled is standard and similar to the one that the points of a Poisson point process are almost surely in general quadratic position; see, e.g. [12] and [17, Proposition 4.1.2].

The proof of Theorem 4.3 is based on the next statement generalising a transformation formula given in [24, p. 314].

Proposition B.1. *Let $L \in \mathcal{L}_k^d$, and let $f\colon L^{k+1} \to \mathbb{R}_+$ be a measurable function. Furthermore, consider strictly monotonic increasing, differentiable functions $r_i\colon [a,\infty) \to \mathbb{R}_+$, $i = 0,\dots,k$, with an arbitrary real number a. Then we have*

$$\begin{aligned}
\int_L \cdots \int_L f(x_0,\dots,x_k)\lambda_d(\mathrm{d}x_0)\cdots\lambda_d(\mathrm{d}x_k) \\
= k! \int_L \int_a^\infty \prod_{i=0}^k (r_i(t)^{k-1}\dot{r}_i(t)) \\
\times \int_{\mathbb{S}^{d-1}\cap L} \cdots \int_{\mathbb{S}^{d-1}\cap L} f(y+r_0(t)u_0,\dots,y+r_k(t)u_k) \\
\times \Delta_k\left(\frac{1}{\dot{r}_0(t)}u_0,\dots,\frac{1}{\dot{r}_k(t)}u_k\right) \\
\times \sigma_L(\mathrm{d}u_0)\cdots\sigma_L(\mathrm{d}u_k)\,\mathrm{d}t\,\mathcal{H}^k(\mathrm{d}y),
\end{aligned}$$

where $\dot{r}_i$ is the derivative of the function r_i, $i = 0,\dots,k$.

Proof. We will only prove this proposition for $L = \mathbb{R}^k \subset \mathbb{R}^d$. The statement then follows by introducing an appropriate coordinate system on L. Define a mapping

$$T\colon \mathbb{R}^k \times [a,\infty) \times \mathbb{S}^{k-1} \times \cdots \times \mathbb{S}^{k-1} \to (\mathbb{R}^k)^{k+1},$$
$$(y,t,u_0,\dots,u_k) \mapsto \begin{pmatrix} y+r_0(t)u_0 \\ \vdots \\ y+r_k(t)u_k \end{pmatrix}.$$

It is easy to see that T is injective. We have to show that the determinant of the Jacobian of T is given by

$$D = D(y,t,u_0,\dots,u_k) = k! \prod_{i=0}^k (r_i(t)^{k-1}\dot{r}_i(t))\Delta_k\left(\frac{1}{\dot{r}_0(t)}u_0,\dots,\frac{1}{\dot{r}_k(t)}u_k\right).$$

Assume that the unit vectors u_i are given in spherical coordinates, and let $\dot{u}_i$ denote the derivative of u_i with respect to these coordinates. Writing E_k for the k-dimensional unit matrix we obtain

$$D = \begin{vmatrix} E_k & \dot{r}_0(t)u_0 & r_0(t)\dot{u}_0 & 0 & \cdots & 0 \\ E_k & \dot{r}_1(t)u_1 & 0 & r_1(t)\dot{u}_1 & \cdots & 0 \\ \vdots & \vdots & \vdots & \vdots & \ddots & \vdots \\ E_k & \dot{r}_k(t)u_k & 0 & 0 & \cdots & r_k(t)\dot{u}_k \end{vmatrix}.$$

https://doi.org/10.1239/aap/1222868179 Published online by Cambridge University Press

For $\tilde{D} = (\prod_{i=0}^{k} 1/r_i(t))^{k-1} D$, this leads to

$$\tilde{D}^2 = \begin{vmatrix} E_k & E_k & \cdots & E_k \\ \dot{r}_0(t)u_0^t & \dot{r}_1(t)u_1^t & \cdots & \dot{r}_k(t)u_k^t \\ \dot{u}_0^t & 0 & \cdots & 0 \\ 0 & \dot{u}_1^t & \cdots & 0 \\ \vdots & \vdots & \ddots & \vdots \\ 0 & 0 & \cdots & \dot{u}_k^t \end{vmatrix} \begin{vmatrix} E_k & \dot{r}_0(t)u_0 & \dot{u}_0 & 0 & \cdots & 0 \\ E_k & \dot{r}_1(t)u_1 & 0 & \dot{u}_1 & \cdots & 0 \\ \vdots & \vdots & \vdots & \vdots & \ddots & \vdots \\ E_k & \dot{r}_k(t)u_k & 0 & 0 & \cdots & \dot{u}_k \end{vmatrix}$$
$$= \begin{vmatrix} (k+1)E_k & \sum \dot{r}_i(t)u_i & \dot{u}_0 & \dot{u}_1 & \cdots & \dot{u}_k \\ \sum \dot{r}_i(t)u_i^t & \sum \dot{r}_i(t)^2 & 0 & 0 & \cdots & 0 \\ \dot{u}_0^t & 0 & E_{k-1} & 0 & \cdots & 0 \\ \dot{u}_1^t & 0 & 0 & E_{k-1} & \cdots & 0 \\ \vdots & \vdots & \vdots & & \ddots & \vdots \\ \dot{u}_k^t & 0 & 0 & 0 & \cdots & E_{k-1} \end{vmatrix}.$$

Now we will use the formula $|A| = |B||A_{22}|$, where

$$A = \begin{pmatrix} A_{11} & A_{12} \\ A_{21} & A_{22} \end{pmatrix} \quad \text{and} \quad B = A_{11} - A_{12}A_{22}^{-1}A_{21},$$

if the matrix A is symmetric and A_{22}^{-1} exists. In our case we have $A_{22} = E_{(k+1)(k-1)}$. Furthermore, note that $E_k - \dot{u}_i\dot{u}_i^t = u_i u_i^t$, as the matrix $u_i\dot{u}_i$ is orthogonal. Using this relation, we obtain

$$\begin{aligned} \tilde{D}^2 &= \begin{vmatrix} (k+1)E_k - \sum \dot{u}_i\dot{u}_i^t & \sum \dot{r}_i(t)u_i \\ \sum \dot{r}_i(t)u_i^t & \sum \dot{r}_i(t)^2 \end{vmatrix} \\ &= \begin{vmatrix} \sum u_i u_i^t & \sum \dot{r}_i(t)u_i \\ \sum \dot{r}_i(t)u_i^t & \sum \dot{r}_i(t)^2 \end{vmatrix} \\ &= \left| \begin{pmatrix} u_0 & \cdots & u_k \\ \dot{r}_0(t) & \cdots & \dot{r}_k(t) \end{pmatrix} \begin{pmatrix} u_0^t & \dot{r}_0(t) \\ \vdots & \vdots \\ u_k^t & \dot{r}_k(t) \end{pmatrix} \right| \\ &= (k!)^2 \prod_{i=0}^{k} \dot{r}_i(t)^2 \Delta_k^2\left(\frac{1}{\dot{r}_0(t)}u_0, \ldots, \frac{1}{\dot{r}_k(t)}u_k\right), \end{aligned}$$

which completes the proof.

Proof of Theorem 4.3. We will concentrate on the case in which $1 \le k \le d-1$. The proofs for the cases in which $k = 0$ and $k = d$ work similarly. Write $m = d - k$. Using the definition of μ_k, the Slivnyak–Mecke formula (see, e.g. [4, pp. 186–187]), and (3.1), we obtain

$$\begin{aligned} \mu_k &= \mathrm{E}\Bigg[\sum_{F \in \mathcal{S}_k(X)} \mathcal{H}^k(F \cap [0,1]^d)\Bigg] \\ &= \frac{1}{(m+1)!}\mathrm{E}\Bigg[\sum_{s_0,\ldots,s_m \in \Phi}^{\neq} \int \mathbf{1}\{y \in [0,1]^d \cap F(s_0,\ldots,s_m,\Phi)\}\mathcal{H}^k(\mathrm{d}y)\Bigg] \end{aligned}$$

https://doi.org/10.1239/aap/1222868179 Published online by Cambridge University Press

$$= \frac{\lambda^{m+1}}{(m+1)!} \int_0^\infty \cdots \int_0^\infty \int_{\mathbb{R}^d} \cdots \int_{\mathbb{R}^d} \int \mathrm{E}[\mathbf{1}\{y \in [0,1]^d \cap F((x_0, r_0), \dots, (x_m, r_m), \Phi)\}] \times \mathcal{H}^k(\mathrm{d}y)\lambda_d(\mathrm{d}x_0) \cdots \lambda_d(\mathrm{d}x_m)\rho(\mathrm{d}r_0) \cdots \rho(\mathrm{d}r_m),$$

where '$\sum^{\neq}$' denotes summation over pairwise distinct points of Φ. Denote the affine hull of $F((x_0, r_0), \dots, (x_m, r_m), \Phi)$ by $G((x_0, r_0), \dots, (x_m, r_m))$. Then,

$$\mu_k = \frac{\lambda^{m+1}}{(m+1)!} \times \int_0^\infty \cdots \int_0^\infty \int_{\mathbb{R}^d} \cdots \int_{\mathbb{R}^d} \int \mathbf{1}\{y \in [0,1]^d \cap G((x_0, r_0), \dots, (x_m, r_m))\} \times p(\mathrm{pow}(y, (x_0, r_0)))\mathcal{H}^k(\mathrm{d}y)\lambda_d(\mathrm{d}x_0) \cdots \lambda_d(\mathrm{d}x_m) \times \rho(\mathrm{d}r_0) \cdots \rho(\mathrm{d}r_m).$$

Using the affine Blaschke–Petkantschin formula (see, e.g. [23, Satz 6.1.5]), we obtain

$$\mu_k = \frac{\lambda^{m+1}}{(m+1)!} c_{dm}(m!)^k \times \int_0^\infty \cdots \int_0^\infty \int_{\mathcal{E}_m^d} \int_E \cdots \int_E \int \mathbf{1}\{y \in [0,1]^d \cap G((x_0, r_0), \dots, (x_m, r_m))\} \times p(\mathrm{pow}(y, (x_0, r_0)))\mathcal{H}^k(\mathrm{d}y) \times \Delta_m^k(x_0, \dots, x_m)\mathcal{H}^m(\mathrm{d}x_0) \cdots \mathcal{H}^m(\mathrm{d}x_m) \times \mu_m(\mathrm{d}E)\rho(\mathrm{d}r_0) \cdots \rho(\mathrm{d}r_m).$$

It is well known that there exist unique invariant measures ν_m on $\mathcal{L}_m^d$ and η_m on $\mathcal{E}_m^d$ such that $\nu_m(\mathcal{L}_m^d) = 1$ and that, for any measurable function $f: \mathcal{E}_m^d \to \mathbb{R}_+$,

$$\int_{\mathcal{E}_m^d} f(E)\eta_m(\mathrm{d}E) = \int_{\mathcal{L}_m^d} \int_{L^\perp} f(L+y)\mathcal{H}^{d-m}(\mathrm{d}y)\nu_m(\mathrm{d}L) = \int_{SO_d} \int_{L_0^\perp} f(\vartheta(y + L_0))\mathcal{H}^{d-m}(\mathrm{d}y)\nu(\mathrm{d}\vartheta), \tag{B.2}$$

where $L_0 \in \mathcal{L}_m^d$ is a fixed linear subspace of $\mathbb{R}^d$ (see, e.g. [23, Satz 1.3.3, Satz 1.3.4, and p. 29]).

For an arbitrary subspace $L \in \mathcal{L}_m^d$ and $(x_0, r_0), \dots, (x_m, r_m) \in \vartheta L \times \mathbb{R}_+$, we find a unique point $z = z((x_0, r_0), \dots, (x_m, r_m)) \in \vartheta L$ such that $G((x_0, r_0), \dots, (x_m, r_m)) = z + \vartheta L^\perp$. Furthermore, $z((x + x_0, r_0), \dots, (x + x_m, r_m)) = x + z((x_0, r_0), \dots, (x_m, r_m))$ for any $x \in \vartheta L^\perp$.

Now fix a subspace $L \in \mathcal{L}_m^d$ and apply (B.2), which yields

$$\mu_k = \frac{\lambda^{m+1}}{(m+1)!} c_{dm}(m!)^k \times \int_0^\infty \cdots \int_0^\infty \int_{SO_d} \int_{\vartheta L^\perp} \int_{\vartheta L} \cdots \int_{\vartheta L} \int p(\mathrm{pow}(y, (x + x_0, r_0))) \times \mathbf{1}\{y \in [0,1]^d \cap x + z((x_0, r_0), \dots, (x_m, r_m)) + \vartheta L^\perp\} \times \mathcal{H}^k(\mathrm{d}y)\Delta_m^k(x_0, \dots, x_m)\mathcal{H}^m(\mathrm{d}x_0) \cdots \mathcal{H}^m(\mathrm{d}x_m)\mathcal{H}^k(\mathrm{d}x)\nu(\mathrm{d}\vartheta)\rho(\mathrm{d}r_0) \cdots \rho(\mathrm{d}r_m).$$

https://doi.org/10.1239/aap/1222868179 Published online by Cambridge University Press

Now the change of coordinates introduced in Proposition B.1 with $z = z(s_0, \dots, s_m)$, $t = \mathrm{pow}(z, s_0)$, and $r_i(t) = (t + r_i^2)^{1/2}$ yields

$$\mu_k = \frac{\lambda^{m+1} c_{dm} (m!)^{k+1}}{2(m+1)!} \int_0^\infty \cdots \int_0^\infty \int_{-\min_i r_i^2}^\infty \prod_{i=0}^m (t + r_i^2)^{(m-2)/2}$$
$$\times \int_{SO_d} \int_{\vartheta L^\perp} \int_{\vartheta L} \int p(t + \|x + z - y\|^2)$$
$$\times \mathbf{1}\{y \in [0,1]^d \cap x + z + \vartheta L^\perp\} \mathcal{H}^k(\mathrm{d}y) \mathcal{H}^m(\mathrm{d}z) \mathcal{H}^k(\mathrm{d}x)$$
$$\times \int_{\mathbb{S}^{d-1} \cap \vartheta L} \cdots \int_{\mathbb{S}^{d-1} \cap \vartheta L} \Delta_m^{k+1}((t + r_0^2)^{1/2} u_0, \dots, (t + r_m^2)^{1/2} u_m)$$
$$\times \sigma_L(\mathrm{d}u_0) \cdots \sigma_L(\mathrm{d}u_m) \nu(\mathrm{d}\vartheta)\, \mathrm{d}t \rho(\mathrm{d}r_0) \cdots \rho(\mathrm{d}r_m).$$

Substitute $(u_0, \dots, u_m, z, x)$ by $(\vartheta u_0, \dots, \vartheta u_m, \vartheta z, \vartheta x)$ and use the fact that $\Delta_m(\cdot)$ and $\mathcal{H}^i(\cdot)$ are invariant under rotations. This yields

$$\mu_k = \frac{\lambda^{m+1} c_{dm} (m!)^{k+1}}{2(m+1)!} \int_0^\infty \cdots \int_0^\infty \int_{-\min_i r_i^2}^\infty \prod_{i=0}^m (t + r_i^2)^{(m-2)/2}$$
$$\times \int_{SO_d} \int_{L^\perp} \int_L \int p(t + \|\vartheta(x + z) - y\|^2)$$
$$\times \mathbf{1}\{y \in [0,1]^d \cap \vartheta(x + z + L^\perp)\} \mathcal{H}^k(\mathrm{d}y) \mathcal{H}^m(\mathrm{d}z) \mathcal{H}^k(\mathrm{d}x) \nu(\mathrm{d}\vartheta)$$
$$\times \int_{\mathbb{S}^{d-1} \cap L} \cdots \int_{\mathbb{S}^{d-1} \cap L} \Delta_m^{k+1}((t + r_0^2)^{1/2} u_0, \dots, (t + r_m^2)^{1/2} u_m)$$
$$\times \sigma_L(\mathrm{d}u_0) \cdots \sigma_L(\mathrm{d}u_m)\, \mathrm{d}t \rho(\mathrm{d}r_0) \cdots \rho(\mathrm{d}r_m).$$

By the change of variables $y_0 = y - \vartheta(x + z) \in \vartheta L^\perp$ we get

$$\mu_k = \frac{\lambda^{m+1} c_{dm} (m!)^{k+1}}{2(m+1)!} \int_0^\infty \cdots \int_0^\infty \int_{-\min_i r_i^2}^\infty \prod_{i=0}^m (t + r_i^2)^{(m-2)/2}$$
$$\times \int_{SO_d} \int_{L^\perp} \int_L \int p(t + \|y_0\|^2)\, \mathbf{1}\{y_0 + \vartheta(x + z) \in [0,1]^d \cap \vartheta(x + z + L^\perp)\}$$
$$\times \mathcal{H}^k(\mathrm{d}y_0) \mathcal{H}^m(\mathrm{d}z) \mathcal{H}^k(\mathrm{d}x) \nu(\mathrm{d}\vartheta)$$
$$\times \int_{\mathbb{S}^{d-1} \cap L} \cdots \int_{\mathbb{S}^{d-1} \cap L} \Delta_m^{k+1}((t + r_0^2)^{1/2} u_0, \dots, (t + r_m^2)^{1/2} u_m)$$
$$\times \sigma_L(\mathrm{d}u_0) \cdots \sigma_L(\mathrm{d}u_m)\, \mathrm{d}t \rho(\mathrm{d}r_0) \cdots \rho(\mathrm{d}r_m).$$

For fixed $y_0 \in \vartheta L^\perp$, we have

$$\int_{L^\perp} \int_L \mathbf{1}\{y_0 + \vartheta(x + z) \in [0,1]^d \cap \vartheta(x + z + L^\perp)\} \mathcal{H}^m(\mathrm{d}z) \mathcal{H}^k(\mathrm{d}x)$$
$$= \int_{L^\perp} \int_L \mathbf{1}\{y_0 + x + z \in [0,1]^d\} \mathcal{H}^m(\mathrm{d}z) \mathcal{H}^k(\mathrm{d}x)$$
$$= 1,$$

and, therefore,

$$\mu_k = \frac{\lambda^{m+1}}{2(m+1)!} c_{dm} (m!)^{k+1} \\ \times \int_0^\infty \cdots \int_0^\infty \int_{-\min_i r_i^2}^\infty \prod_{i=0}^m (t + r_i^2)^{(m-2)/2} \int_{L^\perp} p(t + \|y_0\|^2) \mathcal{H}^k(\mathrm{d}y_0) \\ \times \int_{\mathbb{S}^{d-1}\cap L} \cdots \int_{\mathbb{S}^{d-1}\cap L} \Delta_m^{k+1}((t + r_0^2)^{1/2} u_0, \dots, (t + r_m^2)^{1/2} u_m) \\ \times \sigma_L(\mathrm{d}u_0) \cdots \sigma_L(\mathrm{d}u_m)\, \mathrm{d}t \rho(\mathrm{d}r_0) \cdots \rho(\mathrm{d}r_m),$$

which, introducing spherical coordinates $y_0 = s^{1/2} u$ in $L^\perp$, reads

$$\mu_k = \frac{\lambda^{m+1} c_{dm} (m!)^{k+1}}{4(m+1)!} \sigma_k \\ \times \int_0^\infty \cdots \int_0^\infty \int_{-\min_i r_i^2}^\infty \prod_{i=0}^m (t + r_i^2)^{(m-2)/2} \int_0^\infty p(t+s) s^{(k-2)/2}\, \mathrm{d}s \\ \times \int_{\mathbb{S}^{d-1}\cap L} \cdots \int_{\mathbb{S}^{d-1}\cap L} \Delta_m^{k+1}((t + r_0^2)^{1/2} u_0, \dots, (t + r_m^2)^{1/2} u_m) \\ \times \sigma_L(\mathrm{d}u_0) \cdots \sigma_L(\mathrm{d}u_m)\, \mathrm{d}t \rho(\mathrm{d}r_0) \cdots \rho(\mathrm{d}r_m).$$

Proofs of Theorem 4.4 and Theorem 4.5. Again, we restrict attention to the case in which $0 < k < d$. With respect to the Palm probability measure of M_k, the origin is almost surely contained in a unique k-face $F_k(0) = F(S_{k,0}, \dots, S_{k,m}, \Phi)$ generated by the spheres $S_{k,0}, \dots, S_{k,m}$. Write $G_k(0)$ for the affine hull of $F_k(0)$ and choose $v \in G_k(0) \cap \mathbb{S}^{d-1}$ and $l \geq 0$. Then $lv \in F_k(0)$ holds if and only if $\mathrm{pow}(lv, S_{k,0}) \leq \mathrm{pow}(lv, (x, r))$ for all $(x, r) \in \Phi$. Hence,

$$\mathcal{H}^k(F_k(0)) = \int_0^\infty l^{k-1} \int_{\mathbb{S}^{d-1}\cap G_k(0)} \mathbf{1}\{\mathrm{pow}(lv, S_{k,0}) \leq \mathrm{pow}(lv, (x, r)),\ (x, r) \in \Phi\} \\ \times \sigma_{G_k(0)}(\mathrm{d}v)\, \mathrm{d}l.$$

Let $h \colon \mathbb{R}_+ \to \mathbb{R}_+$ be a measurable function. Then a calculation similar to the proof of Theorem 4.3 yields

$$\mu_k \mathrm{E}^0_{M_k}[h(\mathcal{H}^k(F_k(0)))] \\ = \frac{\lambda^{m+1}}{4(m+1)!} c_{dm} (m!)^{k+1} \int_0^\infty \cdots \int_0^\infty \int_{-\min_i r_i^2}^\infty \prod_{i=0}^m (t + r_i^2)^{(m-2)/2} \int_0^\infty p(t+s) s^{(k-2)/2} \\ \times \int_{\mathbb{S}^{d-1}\cap L^\perp} \int_{SO_d} \mathrm{E}[h(\tilde{A}_{\vartheta L^\perp}(t, s, \vartheta u, \Phi^{s+t}))] \nu(\mathrm{d}\vartheta) \sigma_{L^\perp}(\mathrm{d}u)\, \mathrm{d}s \\ \times \int_{\mathbb{S}^{d-1}\cap L} \cdots \int_{\mathbb{S}^{d-1}\cap L} \Delta_m^{k+1}((t + r_0^2)^{1/2} u_0, \dots, (t + r_m^2)^{1/2} u_m) \\ \times \sigma_L(\mathrm{d}u_0) \cdots \sigma_L(\mathrm{d}u_m)\, \mathrm{d}t \rho(\mathrm{d}r_0) \cdots \rho(\mathrm{d}r_m),$$

https://doi.org/10.1239/aap/1222868179 Published online by Cambridge University Press

where $\Phi^t = \Phi \cap \{(x, r) \colon \operatorname{pow}(0, (x, r)) > t\}$ and

$$\tilde{A}_L(t, s, u, \eta) = \int_0^\infty l^{k-1} \int_{\mathbb{S}^{d-1} \cap L} \mathbf{1}\{\tau(l, t, s, u, v) \le \operatorname{pow}(lv, (x, r)), (x, r) \in \eta\} \sigma_L(\mathrm{d}v)\, \mathrm{d}l$$

with $\tau(l, t, s, u, v) = l^2 + t + s - 2ls^{1/2}\langle u, v\rangle$. Now, by a short calculation using the invariance under rotations of Φ^{s+t} and $\sigma_{L^\perp}$, we obtain

$$\begin{aligned}
&\mu_k \, \mathrm{E}^0_{M_k}[h(\mathcal{H}^k(F_k(0)))] \\
&\quad = \frac{\lambda^{m+1}}{4(m+1)!} c_{dm} (m!)^{k+1} \sigma_k \\
&\qquad \times \int_0^\infty \cdots \int_0^\infty \int_{-\min_i r_i^2}^\infty \prod_{i=0}^m (t + r_i^2)^{(m-2)/2} \\
&\qquad \times \int_0^\infty p(t+s) s^{(k-2)/2} \, \mathrm{E}[h(\tilde{A}_{L^\perp}(t, s, u, \Phi^{s+t}))] \, \mathrm{d}s \\
&\qquad \times \int_{\mathbb{S}^{d-1} \cap L} \cdots \int_{\mathbb{S}^{d-1} \cap L} \Delta_m^{k+1}((t + r_0^2)^{1/2} u_0, \ldots, (t + r_m^2)^{1/2} u_m) \\
&\qquad\qquad \times \sigma_L(\mathrm{d}u_0) \cdots \sigma_L(\mathrm{d}u_m) \, \mathrm{d}t \rho(\mathrm{d}r_0) \cdots \rho(\mathrm{d}r_m).
\end{aligned}$$

For the proof of Theorem 4.5, choose $h(x) = x$ and check that

$$p(s+t)\, \mathrm{P}(\tau(l, t, s, u, v) \le \operatorname{pow}(lv, (x, r)),\ (x, r) \in \Phi^{s+t}) = \xi(l, s+t, \tau(l, t, s, u, v)).$$

The formula for γ_k is obtained using (2.2) and $h(x) = x^{-1}$.

Proof of Theorem 5.1. The theorem easily follows by observing that in every realisation of Φ the power $\operatorname{pow}(y, (x, vr))$ at any point y from any nucleus x of Φ_v tends to $\|y - x\|^2$, the distance function generating the Voronoi tessellation $L^V(\hat{\Phi})$.

Proof of Theorem 5.2. Let $\phi = \{(x_i, r_i)\}$ be a configuration of Φ, let $\phi_v = \{(x, vr) \colon (x, r) \in \phi\}$, and let $\tilde{\phi} = \{x \colon (x, s) \in \phi\}$. Given W, ϕ, and $y \in W$, consider

$$\begin{aligned}
D &= D(v, \phi) \\
&= \operatorname{pow}(y, (x, vr)) - \operatorname{pow}(y, (\tilde{x}(y), vs)) \\
&= \|y - x\|^2 - \|y - \tilde{x}(y)\| + v^2(s^2 - r^2),
\end{aligned} \tag{B.3}$$

where $\tilde{x}(y)$ is (possibly one of) the point(s) of $\tilde{\phi}$ closest to y. When $x = \tilde{x} \in \tilde{\phi}$ in (B.3), then $D = \|y - \tilde{x}\|^2 - \|y - \tilde{x}(y)\|^2 \ge 0$. When $(x, r) \in \phi$, $r < s$, and $\|y - x\| \ge \|y - \tilde{x}(y)\|$,

$$D \ge \|y - x\|^2 - \|y - \tilde{x}(y)\|^2 \ge 0.$$

Finally, let m be the maximal value of the weights of the points $(x, r) \in \phi$ such that $r < s$ and $\|y - x\| < \|y - \tilde{x}(y)\|$. By local finiteness, there is only a finite number of such points, implying that $m < s$. Then

$$D \ge -\|y - \tilde{x}(y)\|^2 + v^2(s^2 - m^2),$$

which is positive for all $v^2 > \|y - \tilde{x}(y)\|^2/(s^2 - m^2)$. Thus, we have shown that, for such large v, the minimum power at y is provided by the nucleus $(\tilde{x}(y), vs)$, so that y belongs to the

Laguerre cell $C((\tilde{x}(y), vs), \phi_v)$ and also implying that y belongs to the Voronoi cell $C^V(\tilde{x}, \tilde{\phi})$ constructed with respect to nuclei set $\tilde{\phi}$. Thus, for all $v > v_0$, all the points in W belong to the Voronoi cells centred at their closest $\tilde{\phi}$-points. As v_0, we may take the square root of the ratio of the maximal diameter d of all the cells $C^V(\tilde{x}, \phi_v)$ intersecting W to s^2 minus the squared maximum radius among all non-$\tilde{\phi}$-points in the d-neighbourhood of W.

Acknowledgements

Most of the results presented in this work are part of CL's PhD thesis written at the Fraunhofer ITWM Kaiserslautern and the University Karlsruhe (TH). CL wishes to thank Günter Last and Katja Schladitz for their support and advice during the work on this thesis. The presentation of the results in the present form was supported by the Swedish Foundation for Strategic Research (SSF) through the Gothenburg Mathematical Modelling Centre (GMMC).

SZ would like to thank Franz Aurenhammer for introducing him to Laguerre tessellations.

References

[1] Ash, P. and Bolker, E. (1986). Generalized Dirichlet tessellations. *Geometriae Dedicata* **20,** 230–243.

[2] Aurenhammer, F. (1987). A criterion for the affine equivalence of cell complexes in $\mathbb{R}^d$ and convex polyhedra in $\mathbb{R}^{d+1}$. *Discrete Computational Geometry* **2,** 49–64.

[3] Aurenhammer, F. (1987). Power diagrams: properties, algorithms and applications. *SIAM J. Comput.* **16,** 78–96.

[4] Barndorff-Nielsen, O., Kendall, W. and van Lieshout, M. (1999). *Stochastic Geometry Likelihood and Computation*. Chapman & Hall/CRC, Boca Raton, FL.

[5] Baumstark, V. and Last, G. (2007). Some distributional results for Poisson–Voronoi tessellations. *Adv. Appl. Prob.* **39,** 16–40.

[6] Blaschke, W. (1929). *Vorlesungen über Differentialgeometrie und geometrische Grundlagen von Einsteins Relativitätstheorie*. Springer, Berlin.

[7] Boissonnat, J.-D. and Yvinec, M. (1998). *Algorithmic Geometry*. Cambridge University Press.

[8] Coxeter, H. S. M. (1969). *Introduction to Geometry*. John Wiley, New York.

[9] Fischer, W., Koch, E. and Hellner, E. (1971). Zur Berechnung von Wirkungsbereichen in Strukturen anorganischer Verbindungen. *Neues Jahrbuch für Mineralogie Monatshefte* **1971,** 227–237.

[10] Heinrich, L. (1998). Contact and chord length distribution of a stationary Voronoi tessellation. *Adv. Appl. Prob.* **30,** 603–618.

[11] Imai, H., Iri, M. and Murota, K. (1985). Voronoi diagram in the Laguerre geometry and its applications. *SIAM J. Comput.* **14,** 93–105.

[12] Lautensack, C. (2007). *Random Laguerre tessellations.* Lautensack, Weiler bei Bingen. Available at http://www.itwm.fhg.de/bv/theses/works/lautensack.

[13] Mecke, J. (1984). Parametric representation of mean values for stationary random mosaics. *Math. Operat. Statist. Ser. Statist.* **3,** 437–442.

[14] Miles, R. E. (1971). Isotropic random simplices. *Adv. Appl. Prob.* **3,** 353–382.

[15] Molchanov, I. (2005). *Theory of Random Sets*. Springer, Berlin.

[16] Møller, J. (1989). Random tessellations in $\mathbb{R}^d$. *Adv. Appl. Prob.* **21,** 37–73.

[17] Møller, J. (1992). Random Johnson–Mehl tessellations. *Adv. Appl. Prob.* **24,** 814–844.

[18] Møller, J. (1994). *Lectures on Random Voronoi Tessellations* (Lecture Notes Statist. **87**). Springer, New York.

[19] Muche, L. and Stoyan, D. (1992). Contact and chord length distributions of the Poisson–Voronoi tessellation. *J. Appl. Prob.* **29,** 467–471.

[20] Okabe, A., Boots, B., Sugihara, K. and Chiu, S. N. (2000). *Spatial Tessellations – Concepts and Applications of Voronoi Diagrams*, 2nd edn. John Wiley, Chichester.

[21] Schlottmann, M. (1993). Periodic and quasi-periodic Laguerre tilings. *Internat. J. Modern Phys. B* **7,** 1351–1363.

[22] Schneider, R. (1993). *Convex Bodies: The Brunn–Minkowski Theory*. Cambridge University Press.

[23] Schneider, R. and Weil, W. (1992). *Integralgeometrie*. Teubner, Stuttgart.

[24] Schneider, R. and Weil, W. (2000). *Stochastische Geometrie*. Teubner, Leipzig.